

RESEARCH PAPER



Pneumonia infection in mice reveals the involvement of the *feoA* gene in the pathogenesis of *Acinetobacter baumannii*

Laura Álvarez-Fraga[†], Juan C. Vázquez-Ucha[†], Marta Martínez-Gutián[†], Juan A. Vallejo, Germán Bou, Alejandro Beceiro[‡], and Margarita Poza[‡]

Servicio de Microbiología, Instituto de Investigación Biomédica (INIBIC), Complejo Hospitalario Universidade (CHUAC), Universidad da Coruña (UDC), A Coruña, Spain

ABSTRACT

Acinetobacter baumannii has emerged in the last decade as an important nosocomial pathogen. To identify genes involved in the course of a pneumonia infection, gene expression profiles were obtained from *A. baumannii* ATCC 17978 grown in mouse infected lungs and in culture medium. Gene expression analysis allowed us to determine a gene, the A1S_0242 gene (*feoA*), over-expressed during the pneumonia infection. In the present work, we evaluate the role of this gene, involved in iron uptake. The inactivation of the A1S_0242 gene resulted in an increase susceptibility to oxidative stress and a decrease in biofilm formation, in adherence to A549 cells and in fitness. In addition, infection of *G. mellonella* and pneumonia in mice showed that the virulence of the Δ 0242 mutant was significantly attenuated. Data presented in this work indicated that the A1S_0242 gene from *A. baumannii* ATCC 17978 strain plays a role in fitness, adhesion, biofilm formation, growth, and, definitively, in virulence. Taken together, these observations show the implication of the *feoA* gene plays in the pathogenesis of *A. baumannii* and highlight its value as a potential therapeutic target.

ARTICLE HISTORY

Received 14 July 2017
Revised 14 December 2017
Accepted 19 December 2017




KEYWORDS

Acinetobacter baumannii;
iron uptake; virulence; animal
infection models

Introduction


Acinetobacter baumannii is a Gram negative, non-fermentative, and non-flagellated bacillus. Although it is a normal inhabitant of human skin, intestinal tract and respiratory system, it is currently considered one of the most dangerous opportunistic pathogens. Recently, the World Health Organization included *A. baumannii* in a list of the most important antibiotic resistant pathogens [1]. This bacterium exhibits an excellent ability to develop antibiotic resistance which often results in strains resistant to several antimicrobial families [2,3]. Carbapenems are broadly used to treat *A. baumannii* multiresistant strains; however, resistance to these antimicrobials increased dangerously in the last decade [4]. Similarly, an increment of resistance rates is emerging in the case of last resort antimicrobials such as colistin [5] or tigecycline [6]. Resistance to these antimicrobials has also appeared which lead us to the urgent need to design and evaluate new antimicrobial therapies. In the last decades, the number of hospital outbreaks caused by *A. baumannii* has increased noticeably, partly due to its

multidrug resistance profile [2,7–10]. Although the clinical importance of *A. baumannii* infections has increased, the pathogenicity of this microorganism is sparsely understood. Clinical *A. baumannii* strains exhibit remarkably variations in virulence-associated phenotypes such as motility, adherence, biofilm formation, invasion, iron uptake or cell capsule development among others [11,12]. Some studies have shown that *Acinetobacter* species may reach the human skin and mucosal membranes and then colonize and persist on the host several weeks [13]. Bacterial adherence constitutes an essential step in the colonization process. The ability of the AbH12O-A2 strain, which caused the largest outbreak of *A. baumannii* known worldwide [14–19], to adhere to human cells was one of the main factors involved in its persistence [14]. After adhesion, bacteria may form biofilms that are involved in the persistence of this pathogen in the hospital environment. Some components, such as the staphylococcal biofilm-associated protein (Bap), the CsuA/BABCDE usher-chaperone system or the poly-beta-1-6-N-acetylglucosamine have been

CONTACT Margarita Poza  margarita.poza.dominguez@sergas.es; Alejandro Beceiro  alejandro.beceiro.casas@sergas.es  Servicio de Microbiología, 3ª planta Hospital Universitario, As Xubias S/N, 15006 A Coruña, Spain.

[†]Authors contributed equally to this work.

[‡]Both authors contributed equally to this work (being Alejandro Beceiro and Margarita Poza the both authors).

Supplemental data for this article can be accessed on the publisher's website at  www.tandfonline.com/kvir.

described as involved in the *A. baumannii* biofilm formation and adherence phenotypes [20–24]. The outer membrane protein OmpA plays a role in biofilm formation on abiotic surfaces and has been shown to promote the adherence to eukaryotic host and invasion [25].

Iron is essential for growth in most bacteria due to its redox activity and its role in many vital metabolic reactions, being a cofactor for many bacterial enzymes. Therefore, iron is necessary for bacteria to infect and multiply in tissues and body fluids of the host, playing a relevant role in pathogenesis [26]. Under *in vivo* conditions, iron is not readily available due to cells uptake or sequestration by proteins such as transferrin or lactoferrin, which are components of the innate immunity system that provide defense against pathogens [27,28]. Bacteria encode multiple iron uptake pathways, which provide specificities and affinities for various forms of environmental or host iron. Under iron-limited conditions many invading bacteria respond by producing specific iron chelators, such as siderophores, that remove the iron from the host sources [29–31]. In addition, many bacteria, such as *Escherichia coli*, *Shigella flexneri*, *Helicobacter pylori*, *Campylobacter jejuni* or *Legionella pneumophila*, take up soluble ferrous iron *via* the Feo system [32–40], which is proposed to be the major ferrous iron transport system known in prokaryotes [41]. The Feo system was first identified in *E. coli* [42,43] and it is encoded by the *feoABC* operon. FeoB, a bacterial ferrous iron transporter, is composed of a hydrophilic cytoplasmic domain and an integral membrane domain [44,45]. The C-terminal membrane domain of FeoB is responsible for the formation of a pore in the membrane and the N-terminal contains a GTP-binding domain that regulates the transport activity. The roles of *feoA* and *feoC* remain unknown although *feoC* is predicted to encode for a transcriptional repressor of *feoAB* [32,43,45]. In pathogenic bacteria such as *E. coli*, *H. pylori* or *L. pneumophila*, mutations in the *feoB* gene have been shown to cause deficiency in ferrous iron uptake and virulence [26,33,37–39], including assays emulating conditions encountered during infection of a mammalian host [46]. High-throughput sequencing technologies demonstrated the presence of the Feo system in 50 clinical strains of *A. baumannii* [47].

In the present work, we identified a gene over-expressed during the course of the lung infection of *A. baumannii* in mice, the A1S_0242 gene (*feoA*). We evaluated the role of this gene in fitness, biofilm production, attachment to biotic surfaces, resistance to oxidative stress, and, finally, in the pathogenesis of *A. baumannii* using *Galleria mellonella* and murine pneumonia models.

Results

Genetic context of the *feoA* gene

Transcriptomic analysis revealed a collection of genes differentially expressed in the *A. baumannii* lung infection model. Raw data have been deposited in the GEO database under the accession code GSE100552. Between them, the A1S_0242 (*feoA*) gene was over-expressed in bacteria over the course of the lung infection compared to bacteria grown in LB media, as shown by Illumina (2.67-fold more \pm 0.75) and qRT-PCR (6.34-fold more \pm 2.03) analysis.

The genetic context of this gene was studied. The *feoA* gene, previously annotated in the ATCC 17978 genome (CP018664.1) as a putative ferrous iron transporter protein A containing a *feoA* domain, was found as part of a single operon comprising genes A1S_0242, A1S_0243 and A1S_0244, as assessed by RNA reverse transcription (Figure 1). The A1S_0243 gene was annotated in the ATCC 17978 genome (CP018664.1) as a ferrous transport protein B harboring a *feoB* domain. The A1S_0244 gene was found as a hypothetical protein, with no conserved domains. Real time RT-PCR assays confirmed that both A1S_0243 and A1S_0244 surrounding genes were over-expressed during the lung infection (1.95-fold more \pm 0.36 and 2.78-fold more \pm 0.96, respectively) compared with genes from bacteria grown in LB-flasks.

Moreover, two homologues to the A1S_0242 gene were found in the *A. baumannii* ATCC 17978 genome (CP018664.1). These genes were A1S_3850 and A1S_0652 that showed 53% and 54% of identity with the *feoA* gene, respectively. The A1S_3850 gene, previously annotated in the ATCC 17978 genome as a hypothetical

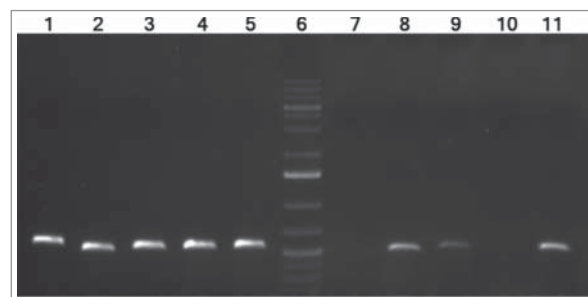


Figure 1. cDNA amplification of genes from the A1S_0242–0244 operon of *A. baumannii* ATCC 17978 strain. The intergenic regions from genes A1S_0242–0243 and A1S_0243–0244 are shown in lanes 8 and 9, respectively. The intergenic regions from genes A1S_0241–0242 and A1S_0244–0245 are shown in lanes 7 and 10, respectively (negative controls). Genomic DNA was used as template for positive control (lanes 1 to 5, respectively). Lanes 5 and 11 show the *gyrB* amplification from DNA and cDNA, respectively (positive controls). Lane 6 shows GeneRuler 1 Kb Plus DNA Ladder (Thermo Fisher Scientific).

protein, is part of a single operon comprising genes A1S_2929, A1S_3850 and A1S_2930 (data not shown). The A1S_2929 and the A1S_2930 genes were annotated as a putative cation efflux system protein and a putative ferrous iron transport protein B containing a *feoB* domain, respectively. The A1S_0652 gene was annotated as a putative ferrous iron transport protein A containing a *feoA* domain followed by the A1S_0653 gene encoding a putative ferrous iron transport protein B. Deeper bioinformatic analysis revealed that the A1S_0652 gene was located in the plasmid pAB3 (GenBank accession number CP012005) of the *A. baumannii* ATCC 17978-mff strain (CP012004.1) while the A1S_3850 was found in the chromosome.

All the publicly available complete genomes of *A. baumannii* were analyzed in order to find the A1S_0242 and the A1S_3850 genes. The A1S_0242 gene was found in the 100% of the 76 *A. baumannii* complete genomes analyzed, while the A1S_3850 gene was located in the 14.5% of them. Similarly, in species such as *A. pittii*, *A. nosocomialis*, *A. soli* or *A. calcoaceticus*, the A1S_3850 gene was occasionally found while the A1S_0242 gene was present in all the analyzed genomes.

The discovery of these two A1S_0242 homologues induced us to investigate possible interactions between those three genes, being the A1S_0242 gene the main objective of our work. Gene knockout mutants of the ATCC 17978 strain lacking the A1S_0242 and A1S_3850 genes were constructed in order to analyze their interaction. Therefore, the isogenic mutant derivatives $\Delta 0242$ and $\Delta 3850$ strains as well as the double mutant $\Delta 0242/\Delta 3850$ strain were obtained. Due to the plasmid location of the A1S_0652 gene, it was not possible to perform a knockout mutant lacking this gene.

The complementation of the A1S_0242 gene with the parental allele ($\Delta 0242$ complemented) was performed through the over-expression of the gene cloned into the pWH1266-Km vector. Data from qRT-PCR analysis revealed that indeed the A1S_0242 was highly over-expressed under the control of the tetracycline promoter compared to its expression in the wild type gene (Table S1). As expected, the $\Delta 0242$ strain, as well as the $\Delta 0242$ strain harboring the empty pWH1266-Km vector ($\Delta 0242 + pWH1266-Km$), revealed no expression of the A1S_0242 gene. Table S1 also shows that there is no expression of the A1S_3850 gene in the $\Delta 3850$ strain and the over-expression of the A1S_3850 gene from the plasmid was confirmed.

Also qRT-PCR analyses were performed in order to investigate the effects of the lack of the A1S_0242 gene on the expression of its homologue genes. Data revealed that when the A1S_0242 gene was absent, the A1S_3850 and the A1S_0652 genes maintained their expression levels (Table 1). Also, the deletion of the A1S_3850 did not vary the expression of the A1S_0242 gene whereas the expression of the A1S_0652 gene increased. In addition, the deletion of both A1S_0242 and A1S_3850 genes revealed a minimal increase in the A1S_0652 expression level, due to the effect of the A1S_3850 gene.

Next, the abilities of the $\Delta 0242$ strain and its isogenic derivative mutants were tested under *in vitro* and *in vivo* conditions to confirm the role of this gene in fitness and virulence. The A1S_3850 mutants were also included in some assays in order to discard its relevance in the pathogenesis of the ATCC 17978 strain.

Effects of the *feoA* gene deletion and vector loading on fitness

To determine whether the deletion of genes A1S_0242 and A1S_3850 affect the bacterial growth rate, growth curve rates were measured in iron-sufficient and iron-restricted media. Determination of the growth rate constant (μ) gives a measure of fitness or replication ability [48]. The growth rates of the $\Delta 0242$ mutant did not show significant differences compared to the wild type strain in presence of iron (Figure 2). However, when the metal chelator 2,2'-bipyridil (BIP) was added to the medium, the mean generation of the $\Delta 0242$ mutant was higher (65 min, $\mu = 0.0105 \pm 0.0003$) with respect to the ATCC 17978 strain (45 min, $\mu = 0.015 \pm 0.0012$), showing significant differences in fitness ($p > 0.05$). In contrast, the deletion of A1S_3850 did not show inhibition of growth compared with the ATCC 17978 parental strain. In agreement with these results, the double mutant $\Delta 0242/\Delta 3850$ showed a growth rate similar to the single mutant $\Delta 0242$ in BIP presence (Figure 2).

Studies of bacterial growth performed with the ATCC 17978 derivative strains carrying the pWH1266-Km vector showed that this plasmid load represents a very relevant biological cost, as shown in Figure S1. These means that all the strains carrying the pWH1266-Km vector showed a significantly lower fitness than the wild type strain. For this reason, complemented strains were not included in assays where the growth rate was limiting.

Table 1. Interaction of genes A1S_0242, A1S_3850 and A1S_0652 measured by qRT-PCR.

	ATCC 17978	$\Delta 0242^*$	$\Delta 3850^*$	$\Delta 0242/\Delta 3850^*$
A1S_0242	1	0	1.02 \pm 0.32	0
A1S_0652	1	0.97 \pm 0.21	2.73 \pm 1.09	1.11 \pm 0.48
A1S_3850	1	0.97 \pm 0.04	0	0

*Data were obtained as a fold-change relative to the ATCC 17978 sample (value 1), using the *rpoB* gene as housekeeping for normalization.

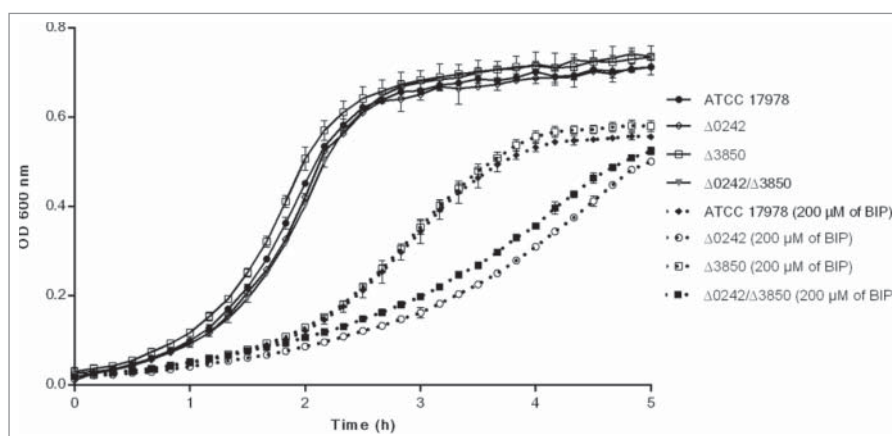


Figure 2. Growth curves of the ATCC 17978 strain and the isogenic mutant derivative strains $\Delta 0242$, $\Delta 3850$ and $\Delta 0242/\Delta 3850$ in presence and absence of the iron chelator 2,2'-bipyridyl (BIP). Data correspond to the mean of three replicates and bars represent the standard deviations.

The *feoA* gene deletion reduces biofilm formation and attachment to eukaryotic cells abilities

The biofilm formation ability was evaluated and the $\Delta 0242$ mutant derivative strain showed a significant decrease (ca. 2,15-fold less, $p = 0.0034$) with respect to the ATCC 17978 parental strain (Figure 3). Complementation of the strain with the parental allele partially restored the biofilm formation phenotype. Deletion of the *A1S_3850* revealed no significant differences in biofilm formation with respect to the wild type strain. Biofilm formation was similar for the single $\Delta 0242$ and the double mutant $\Delta 0242/\Delta 3850$ strains.

As shown in Figure 4, the inactivation of the *A1S_0242* gene led to a reduction in the ability of the *A. baumannii* strain ATCC 17978 to adhere to human alveolar epithelial cells A549 (ca. 4-fold, p value <

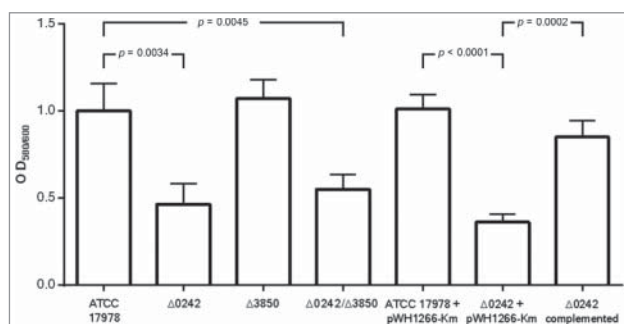


Figure 3. Quantification of biofilm formation by the *A. baumannii* ATCC 17978 strain, the mutant derivative strain $\Delta 0242$, the mutant derivative strain $\Delta 3850$, the double mutant derivative strain $\Delta 0242/\Delta 3850$, the ATCC 17978 harboring the empty vector pWH1266-Km (ATCC 17978 + pWH1266-Km), the mutant derivative strain harboring the empty vector pWH1266-Km ($\Delta 0242$ + pWH1266-Km) and the mutant derivative $\Delta 0242$ over-expressing the *A1S_0242* gene from the pWH1266-Km plasmid ($\Delta 0242$ complemented).

0.0001). In this case, the fitness of the strains was a limiting factor as can be seen in Figure S2, the wild type strain harboring the plasmid (ATCC 17978 + pWH1266-Km) showed an important decrease in biofilm formation ability, compared with the wild type strain (ATCC 17978). The complemented strain ($\Delta 0242$ complemented) partially restored the wild type phenotype loading plasmid (ATCC 17978 + pWH1266-Km), as reflected in Figure S2. As shown in Figure S1, all strains harboring the pWH1266-Km vector resulted in an increase in the lag time and in a lower optical density at the end of growth curve analysis, which indicates a fitness decrease caused by the plasmid metabolic load. Besides, the $\Delta 3850$ strain showed no significant differences with respect to the wild type and the double mutant strain showed similar attachment abilities as the $\Delta 0242$ strain (Figure 4). No invasiveness was detected at 24 h in all cases (data not shown).

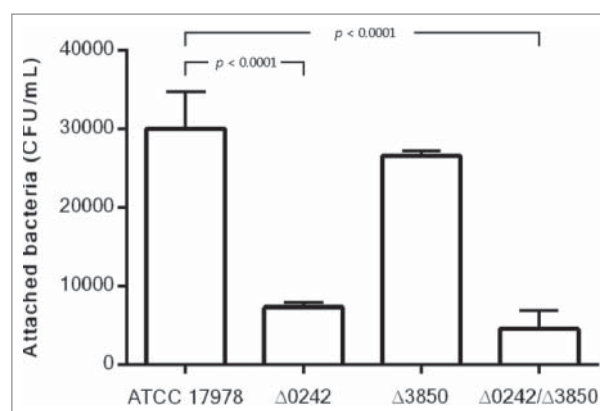


Figure 4. Quantification of bacterial adhesion to A549 cells by the *A. baumannii* ATCC 17978 strain, the mutant derivative strain $\Delta 0242$, the mutant derivative strain $\Delta 3850$ and the double mutant strain $\Delta 0242/\Delta 3850$.

Effects of the *feoA* gene inactivation on susceptibility to oxidative stress

When strains were subjected to reaction oxygen species (ROS) by the addition of paraquat in the presence of 100 μM of the iron chelator 2,2'-bipyridyl (BIP), the $\Delta 0242$ mutant strain showed a MIC to paraquat of 8 mg/L, while the wild type strain ATCC 17978 showed a value of 32 mg/L, which indicates a significant increase in susceptibility to oxidative stress of the mutant strain with respect to the wild type strain (Table 3). No differences were found in the susceptibility to paraquat between the $\Delta 0242$ mutant and the $\Delta 0242/\Delta 3850$ double mutant (MIC of 8 mg/L). In concordance, the $\Delta 3850$ mutant neither showed significant differences with respect to the wild type strain (MIC of 32 mg/L). A slightly higher susceptibility to paraquat in the $\Delta 0242$ mutant was also observed in the medium without limitation of metal availability. Besides, when the strains carried the plasmid pHW1266-Km, the susceptibility to paraquat increased in all cases, due to the fitness loss as explained above (Figure S1). In Table 3 it can be observed that, even taking into account this global increased of susceptibility to paraquat in strains carrying the plasmid, the phenotype of higher susceptibility to oxidative stress in the presence of BIP of the $\Delta 0242$ mutant strain carrying the plasmid ($\Delta 0242+\text{pWH1266-Km}$, MIC of 1 mg/L) was restored in the complemented strain, this showing the same MIC to paraquat as the wild type strain carrying the pWH1266-Km vector (MIC of 4 mg/L).

The *feoA* gene is involved in virulence

In order to explore the role of the *feoA* gene during the course of the *in vivo* infection, experimental animal models were performed in *G. mellonella* and mice.

The *A. baumannii* ATCC 17978 and the $\Delta 0242$, $\Delta 3850$ and $\Delta 0242/\Delta 3850$ derivative mutant strains were tested in the *G. mellonella* infection model. The survival assays (Figure 5) showed that the $\Delta 0242$ and $\Delta 0242/\Delta 3850$ mutant strains were significantly affected in their ability to infect and kill the caterpillars compared with the wild type strain ($p < 0.05$).

These results were in agreement with the mortality rates of *G. mellonella* infected with different inocula of the *A. baumannii* strains (Table 4). Briefly, lethal doses (LD) of the ATCC 17978 strain were similar to those showed by the mutant $\Delta 3850$. Besides, the lethal doses of the mutant $\Delta 0242$ were similar to those found in the $\Delta 0242/\Delta 3850$ mutant strain. The inactivation of the gene A1S_3850 did not affected the virulence ability of the ATCC 17978 strain using this *G. mellonella* infection model. The LD₅₀ of the ATCC 17978 strain and the $\Delta 3850$ mutant was approximately 5-fold lower

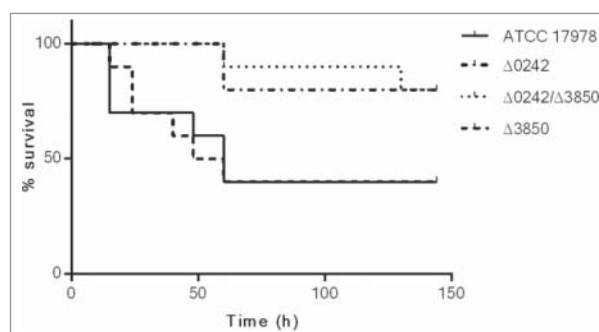


Figure 5. Survival of *Galleria mellonella* larvae ($n = 10$ per group) after infection with *A. baumannii* ATCC 17978, $\Delta 0242$, $\Delta 3850$ and $\Delta 0242/\Delta 3850$ strains. Survival was significantly higher in caterpillars infected with the $\Delta 0242$ mutant than those infected with the wild type strain ($p < 0.05$). No deaths were observed in any of the two control groups (not injected and injected with sterile PBS).

than that of the $\Delta 0242$ and $\Delta 0242/\Delta 3850$ mutant strains at 24 h, and 3.5-fold lower at 144 h. The LD₁₀₀ of the ATCC 17978 strain and the $\Delta 3850$ mutant was approximately 4-fold lower than that of the $\Delta 0242$ and $\Delta 0242/\Delta 3850$ mutant strains at 24 h, and 3-fold lower at 144 h.

The virulence of the ATCC 17978 and $\Delta 0242$ strains was also assessed using a murine pneumonia model by measuring survival time of infected mice. Two groups of 10 mice were intratracheally infected with 5.5×10^7 CFUs/mouse, which means a LD₉₀ of the wild type strain. However, the same dose of the $\Delta 0242$ mutant derivative strain produced only 30% of mortality (Figure 6A). Thus, a significant decrease in virulence using a mouse pneumonia model was observed when the gene A1S_0242 was deleted ($p < 0.01$).

A second model was also performed using an experimental pneumonia model in mice in order to determine the bacterial load in lungs and the frequency of sterile blood cultures (Table 5 and Figure 6B). Data revealed that, in groups inoculated with the ATCC 17978 strain, the bacterial load was approximately 1 log higher than in mice inoculated with the $\Delta 0242$ mutant strain ($p < 0.01$). Besides, the frequency of sterile blood cultures increased up to 75% in the group inoculated with the $\Delta 0242$ mutant strain compared with the mice inoculated with the ATCC 17978 strain (8.4%), ($p < 0.01$). Similarly, the survival time was significantly higher in the group of mice inoculated with the $\Delta 0242$ mutant strain than in the mice harboring the wild type strain ($p < 0.01$).

Discussion

The success of lung infection partly depends on the ability of bacteria to acquire iron, a cofactor needed for

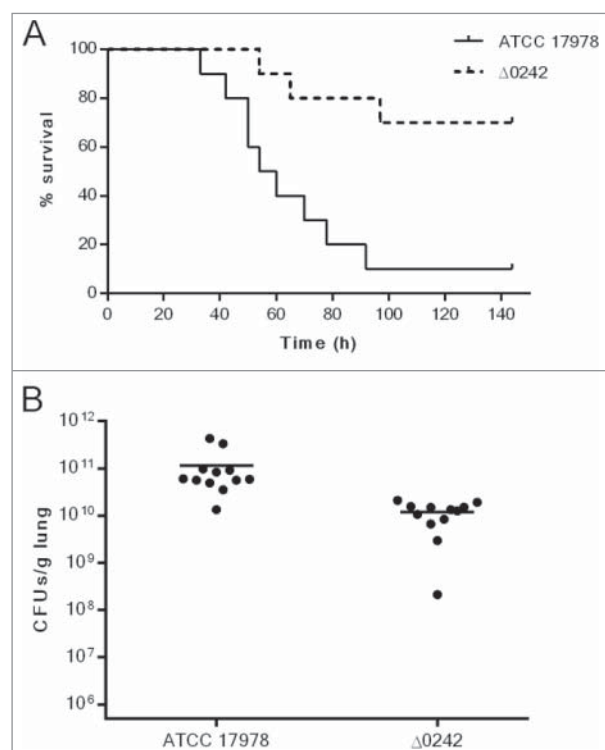


Figure 6. Pneumonia infection in mice. A) Survival of BALB/c ($n = 10$ per group) mice after pneumonia infection with *A. baumannii* ATCC 17978 and $\Delta 0242$ strains. Survival was significantly higher in mice infected with the $\Delta 0242$ mutant ($p < 0.01$). B) Bacterial load determination in lungs of mice infected with the ATCC 17978 strain and the $\Delta 0242$ mutant. Bacterial load ($p < 0.01$) was significantly lower in mice infected with the $\Delta 0242$ mutant.

many enzymatic reactions. Iron is essential for vital functions of bacteria and its presence in the host environment is restricted. This iron restriction constitutes an immune defense mechanism. *A. baumannii* is able to grow under iron-limiting conditions such as those occurred during human infection, however there is scarce information about the iron uptake of this microorganism during the course of the infection. Different studies showed that *A. baumannii* produces siderophores [49] such as the iron chelating agent acinetobactin [18,31,47], the fimsbactin A-F [29] or the baumanoferrin A and B [30] which are required for virulence. In addition, some outer membrane proteins such as OprD and OmpW have been related to iron uptake in *A. baumannii* [50,51]. Recently, a study concerning the gene expression profile of *A. baumannii* revealed that most of the genes hyper-expressed during bacteremia were those involved in iron transport and uptake [52].

At neutral pH and aerobic conditions, the ferric iron Fe^{3+} is insoluble. At this point, bacteria depend on siderophores for the iron uptake, such as acinetobactin, pyoverdinin or enterobactin, previously described in *A. baumannii*, *P. aeruginosa* and *E. coli*,

respectively [53,54], as well as additional molecules with Fe-chelating ability, such as citrate in *P. aeruginosa* [55]. In contrast, in anaerobic conditions, ferrous iron Fe^{2+} is abundant and is captured through uptake systems [56], such as the Feo system. However, a relevant link exists between the Feo system and the citrate-mediated Fe^{3+} acquisition of *P. aeruginosa*. The ferric iron Fe^{3+} chelated by citrate must be reduced to Fe^{2+} prior to its transport into the cytosol by the membrane transporter FeoB. A ferric citrate-specific cytoplasmic membrane transport component is absent in *P. aeruginosa* [57,58]. Similar cooperation between the FeoB transporter and the citrate-promoted Fe acquisition has been suggested in other species, such as *H. pylori* [37] and *Leptospira biflexa* [59]. Genes encoding for the baumanoferrin biosynthetic gene cluster found in *A. baumannii* [30] showed to be homologous to components of the acinetoferrin system, a citrate-based siderophore described in *A. haemolyticus* [60]. However, similar relationships between these siderophores and the Feo system are yet unknown.

Transcriptome analysis of *A. baumannii* ATCC 17978 strain, using RNA isolated from BAL of the infected lungs as starting material, revealed that the A1S_0242 gene (a ferrous iron transporter protein A) was over-expressed during the course of the pneumonia infection. Further analysis of the genome revealed the presence of other two genes (A1S_3850 and A1S_0652) homologues to A1S_0242, both harboring a *feoA* domain. This motivated us to study the genetic context of those genes. Informatic analyses revealed the presence of the A1S_0242 gene in all the complete *A. baumannii* genomes while the A1S_3850 and the A1S_0652 genes were rarely found.

The Feo systems found in *A. baumannii* ATCC 17978 contain in all cases genes similar to the previously described *feoA* and *feoB* genes but lacks the *feoC* gene found in other species. More functional studies related to the A1S_0244 could explain if this gene could act as a *feoAB* repressor in *A. baumannii*. The presence of these three genes containing a *feoA* domain in the strain ATCC 17978 triggered us to study the function of the A1S_0242 (*feoA*) and its interaction with the other two homologue genes (A1S_3850 y A1S_0652). Real time procedures revealed that the lack of A1S_0242 does not vary A1S_0652 and A1S_3850 expression while deletion of A1S_3850 increased the A1S_0652 expression.

In a previous work [61], transcriptional profiles indicated that the A1S_0242 and the A1S_3850 genes expression remained unaltered in biofilm-associated cells when compared to the planktonic cells, while the A1S_0652

gene increased. However, when the transcriptional profile of *A. baumannii* was determined during bacteremia [52], it was recovered that the expression of A1S_0650 and A1S_3850 genes remained unaltered whereas the expression of the A1S_0242 gene increased. Moreover, Eijkelkamp *et al.* [62] studied the transcriptional profiles of the genes of *A. baumannii* under iron limiting conditions. In this case, it was found that the A1S_0242 and A1S_0652 genes were up-regulated under iron limiting conditions while the A1S_3850 gene did not showed any different expression profile.

In this study we report many evidences of the implication of the A1S_0242 gene (*feoA*) in fitness and virulence of *A. baumannii* ATCC 17978. The importance of the *feoA* gene was first evidenced in fitness. The Δ 0242 mutant showed a lower growth rate than the wild-type strain in iron-limited conditions. In contrast the mutants Δ 3850 and Δ 0242/ Δ 3850 did not decreased in growth rates compared with the parental and Δ 0242 strains, respectively, thus minimizing the relevance of the A1S_3850 gene present in the ATCC 17978 strain.

Significant differences were also found in biofilm production or cellular attachment. The deletion of *feoA* demonstrated that this gene was involved in those mechanisms used by *A. baumannii* to colonize and infect the host organs while deletion of the homologue gene A1S_3850 did not show any changes. In agreement with previous results, the mutant Δ 0242 showed a higher susceptibility to oxidative stress than the wild-type strain. Superoxide dismutase plays a key role in metabolizing O_2^- , avoiding reactions that can cause damage and the formation of reactive oxygen species. This enzyme frequently uses Fe as metal cofactor to catalyze the detoxification of superoxide [63]. Therefore, the Δ 0242 mutant strain was more susceptible to the oxidative stress induced by paraquat probably due to decreased superoxide dismutase activity. The Δ 3850 and the double mutant Δ 0242/ Δ 3850 did not showed any effect on biofilm production, cellular attachment or oxidative stress, which once more highlights the important role of the A1S_0242 gene in pathogenesis and indicates the irrelevant role of the A1S_3850 gene in these processes.

Fitness is usually defined as the capacity for survival and reproduction in a particular environment [64], and virulence is defined as the degree of pathogenicity (ability of an agent to cause disease). Most pathogens use of a combination of two properties to cause disease: (i) toxicity, the degree to which a substance causes harm, and (ii) invasiveness, the ability to penetrate into the host and spread [48,65]. In the present study we have proved that fitness is reduced when the *feoA* gene (A1S_0242) is inactivated under iron-limited conditions. Additionally, virulence decreased as judged by the reduced ability of

the mutant Δ 0242 strain to attach to alveolar cells and the increased susceptibility to oxidative stress, which is one of the main antibacterial mechanisms during phagocytosis [66], being all these processes implicated in the pathogenicity of *A. baumannii*. Data indicated that the increase of survival and lethal doses obtained in the *in vivo* models with the Δ 0242 mutant strain is probably due to a double effect or synergy between the fitness lost and the decrease of virulence, caused by a reduced ability to arrest iron from the environment.

Moreover, complementation experiments were performed in order to better demonstrate the role of *feoA* in virulence. Since the load of the pWH1266-Km vector decreases fitness (see Figure S1) not all assays could be performed with the complemented mutants. Accordingly, those assays in which fitness does not play a relevant role, such as biofilm production, were performed including the complemented strains. These assays clearly demonstrated that the complementation is possible and indeed restored the original phenotype. However, those assays where fitness is a limiting factor, such as the *in vivo* assays in animal models, were carried out without the complemented strains.

In a recent screening of genes involved in bacterial survival of *A. baumannii* using a mouse model of bloodstream infection, from a transposon mutant library comprising more than 100,000 mutants, 89 were selected for further studies [46]. Between them, two genes belonged to iron uptake systems, the *fepA* and the *feoB* genes, supporting the role of these systems in the *A. baumannii* pathogenesis [46]. However, no *in vivo* assays were performed on the study to confirm the results. In the present study, the implication of *FeoA* in the pathogenesis of *A. baumannii* was also evidenced using experimental *in vivo* infections that imply the host response. In the first model, previously validated to study *A. baumannii* infections in iron-defective conditions [18,67], caterpillars of *G. mellonella* were infected with the wild-type and mutant strains. Data indicated an impaired in virulence showing a lower capacity to persists and kill the caterpillars in the case of the Δ 0242 strain but not in the case of the Δ 3850 strain, which shows again the lack of implication of the A1S_3850 in pathogenesis. Similarly, in the pneumonia models of infection in mice, the mutant Δ 0242 strain with reduced iron transport functions was less virulent than the wild-type strain. Both assays with invertebrate and vertebrate hosts reflected similar effects. Taken together these observations indicate that the *feoA* gene of *A. baumannii* is essential for the full virulence of this microorganism. However, virulence of *A. baumannii*, using the animal models here presented, was not entirely inhibited, suggesting that other iron transport systems previously described such as *fepA*, acinetobactin, baumanoferrin or fimsbactin [29,30,46,47] are present in the ATCC 17978

strain and should be active when the Feo system is abolished.

In summary, data indicated that the A1S_0242 gene (*feoA*) from *A. baumannii* ATCC 17978 strain, which is involved in iron uptake and that was found as over-expressed during the course of a pneumonia infection, plays a role in adhesion, biofilm formation and resistance to oxidative stress. Definitively, in the present study we demonstrated that the FeoA protein is needed for the full virulence phenotype of the strain ATCC 17978 of *A. baumannii* and that the FeoA-mediated acquisition of iron is essential for the *A. baumannii* pathogenesis.

Material and methods

Bacterial strains

A. baumannii ATCC 17978 and its derivative strains and *E. coli* listed in Table 2 were routinely grown or maintained in Luria-Bertani (LB) or Mueller-Hinton (MH) media with 20% agar added for plates for general purposes. All strains were grown at 37 °C and stored at -80 °C in LB broth containing 10% glycerol. When appropriate, cultures were supplemented with kanamycin (Km) at a final concentration of 50 mg/L (Sigma-Aldrich, #K1377).

Bacterial RNA extraction from murine pneumonia infection

An experimental pneumonia model was used to describe the transcriptome of the ATCC 17978 strain during the course of the infection. BALB/c 9- to 11-week old male mice weighing 25 to 30 g were intratracheally inoculated with approximately 5.5×10^7 CFUs/mouse of exponentially grown cells of the ATCC 17978 strain into mice.

The number of bacteria present in the inoculum was checked by plate counting in LB agar plates. Briefly, mice anesthetized with an oral suspension of sevoflurane (Zoetis, #NADA 141–103) were suspended by their incisors on a board in a semi-vertical position. The efficacy of the intratracheal inoculation was confirmed by using an endoscope on the oral cavity. The trachea was accessed using a blunt-tipped needle for the inoculation of a 40- μ L bacterial suspension made in sterile saline solution and 10% porcine mucin (wt/vol) (Sigma) mixed at a 1:1 ratio. A solution of ketamine (500 μ g/mouse) (Pfizer, #47639/24/15) and medetomidine (15 μ g/mouse) (Domtor, #933ESP) was immediately intraperitoneally injected after inoculation in order to keep the mice at least 20 min in a 30° inclined position. Dead mice in the first 4 h after inoculation were not included in the final analyses. Mice were euthanized with an overdose of thiopental sodium (Sandoz, NDC0781–6160-43) 20 h after inoculation. Then, a bronchoalveolar lavage (BAL) was performed to obtain bacteria suitable for RNA extraction (*in vivo* samples). All mice were maintained in the specific pathogen-free facility at the Technology Training Center of the Hospital of A Coruña (CHUAC, Spain). All experiments were done with the approval of and in accordance with regulatory guidelines and standards set by the Animal Ethics Committee (CHUAC, Spain, project code P82), in accordance with the Helsinki Declaration of 1975. RNA extracted from bacteria grown in LB-flasks ($OD_{600} = 1.0$) at 37°C and 180 rpm was used as experimental control (*in vitro* samples). Total RNA was immediately extracted from both samples using the RNeasy Mini Kit (Qiagen #74104), treated with DNase I (Invitrogen, # 18068015) and purified with RNeasy MinElute Cleanup Kit (Qiagen, #74204). Final concentrations and purity grades of the samples were determined using a BioDrop μ LITE

Table 2. Bacterial strains and plasmids used in this work.

Strain or plasmid	Relevant characteristics	Sources or references
STRAINS		
<i>A. baumannii</i>		
ATCC 17978	Clinical isolate	ATCC
Δ 0242	A1S_0242 gene deletion mutant obtained from the ATCC 17978 strain	This study
ATCC 17978 + pWH1266-Km	ATCC 17978 harboring the empty pWH1266-Km plasmid; Km ^R , Tet ^R	This study
Δ 0242 + pWH1266-Km	Δ 0242 harboring the empty pWH1266-Km plasmid; Km ^R , Tet ^R	This study
Δ 0242 complemented	Δ 0242 harboring the pWH1266-Km-0242 plasmid; Km ^R	This study
Δ 3850	A1S_3850 gene deletion mutant obtained from the ATCC 17978 strain	This study
Δ 3850 + pWH1266-Km	Δ 3850 harboring the empty pWH1266-Km plasmid; Km ^R , Tet ^R	This study
Δ 3850 complemented	Δ 3850 harboring the pWH1266-Km-3850 plasmid; Km ^R	This study
Δ 0242/ Δ 3850	A1S_0242 and A1S_3850 genes deletion double mutant obtained from the ATCC 17978 strain	This study
<i>E. coli</i>		
TG1	Used for DNA recombinant methods	Lucigen
PLASMIDS		
pWH1266-Km	<i>A. baumannii</i> shuttle vector; Km ^R , Tet ^R	Álvarez-Fraga <i>et al.</i> 2016 [68]
pWH1266-Km-0242	pWH1266-Km harboring the A1S_0242 gene; Km ^R	This study
pWH1266-Km-3850	pWH1266-Km harboring the A1S_3850 gene; Km ^R	This study
pMo130	Suicide vector for the construction of <i>A. baumannii</i> isogenic derivative; Km ^R , SacB, XylE	Hamad <i>et al.</i> 2009 [69]

Km^R: kanamycin resistance. Tet^R: tetracycline resistance.

Table 3. Susceptibility to oxidative stress generated by paraquat.

	MICs to paraquat (mg/L)	
	MH broth	MH broth + 100 μ M BIP
ATCC 17978	64	32
Δ 0242	32	8
Δ 3850	64	32
Δ 0242/ Δ 3850	32	8
MICs to paraquat (mg/L) with strains carrying the pWH1266-Km vector		
ATCC 17978 + pWH1266-Km	8	4
Δ 0242 + pWH1266-Km	4	1
Δ 0242 complemented	4	4

(Isogen Life Science) and a Bioanalyzer 2100 (Agilent Technologies Inc.).

Deep sequencing procedures

To characterize the complete transcriptomes of the studied samples, mRNA libraries from *in vivo* and *in vitro* samples obtained as explained above were prepared following the Truseq RNA sample preparation protocols from Illumina Inc. at CIC bioGUNE's genome analysis platform (Derio, Spain). Three biological replicates were studied for each sample.

Read processing and comparisons of gene expression profiles

Fifty nucleotide reads from each mRNA library were obtained using HiScanSQ (Illumina Inc., CIC bioGUNE, Bilbao, Spain). Short reads were aligned against the complete genome of *A. baumannii* ATCC 17978 and plasmids pAB1 and pAB2 (GenBank accession codes: NC_009085.1, NC_009083.1 and NC_009084.1, respectively). The genetic profiles comparison was done at CIC bioGUNE's genome analysis platform (Derio, Spain).

Table 4. Mortality of *G. mellonella* infected with the *A. baumannii* ATCC 17978 and its derivative strains using lethal dose 50 (LD₅₀) and lethal dose 100 (LD₁₀₀).

Strains	Bacterial inoculum (CFUs/larva)						LD ₅₀ 24 h	LD ₁₀₀ 24 h
	8*10 ⁵	2*10 ⁵	8*10 ⁴	2.6*10 ⁴	8*10 ³	2.6*10 ³		
Mortality of larvae (% at 24 h)								
ATCC 17978	100	100	85.7	57.1	42.8	0	1.9*10 ⁴	17*10 ⁴
Δ 0242	100	71.4	57.1	0	0	0	10.5*10 ⁴	63*10 ⁴
Δ 3850	100	100	100	42.8	28.5	0	1.95*10 ⁴	11.7*10 ⁴
Δ 0242/ Δ 3850	100	85.7	57.1	0	0	0	9.3*10 ⁴	53.2*10 ⁴
Mortality of larvae (%) at 144 h								
ATCC 17978	100	100	100	85.7	42.8	0	1*10 ⁴	6*10 ⁴
Δ 0242	100	100	85.7	14.2	0	0	4.35*10 ⁴	18.1*10 ⁴
Δ 3850	100	100	100	100	28.5	0	1.15*10 ⁴	3.05*10 ⁴
Δ 0242/ Δ 3850	100	100	85.7	42.8	0	0	3.4*10 ⁴	16.4*10 ⁴

Table 5. Effect of *feoA* gene (A1S_0242) inactivation over bacterial load in lungs, blood and mice survival.

Treatment group (n)	Bacterial load in lung (mean log ₁₀ CFU/g of lung +/- SD)	% Sterile blood cultures	Mean of survival time (h) of mice
ATCC 17978 (12)	11.04 (+/- 0.35)	8.4%	43.4
Δ 0242 (12)	10.04 (+/- 0.29)	75%	64.1 ^a

^a: Two mice survived at 72 h.

Raw data were deposited in the GEO database under the accession code GSE100552.

Bioinformatic analysis

Genome analyses were done using the basic local Alignment Search Tool of the NCBI (BLAST, <https://blast.ncbi.nlm.nih.gov/Blast.cgi>).

Construction of isogenic deletion derivatives

In the present work, we focused on the study of the A1S_0242 gene. The Δ 0242 isogenic deletion mutant derivative of the ATCC 17978 strain was constructed by deleting a region of the A1S_0242 gene. The suicide vector pMo130 (Genbank: EU862243), was used as described before [68] where upstream and downstream regions flanking the A1S_0242 gene were PCR-amplified and cloned into the pMo130 vector using primers listed in Table S2. The plasmid construction obtained was used to transform ATCC 17978 cells by electroporation [61]. Recombinant colonies representing the first crossover event were selected as previously described [69]. The second crossover event leading to gene knockout was confirmed by PCR using primers listed in Table S2 as described before [68]. The A1S_3850 was found in the genome of the 17978 strain as an A1S_0242 homologue. In order to study its interference with the A1S_0242 gene as well as discard its relevance in pathogenesis, a Δ 3850 isogenic deletion mutant of the ATCC 17978 strain was constructed following the protocol described above and using the primers listed in Table S2. In addition, a double isogenic mutant strain, Δ 0242/ Δ 3850, was performed following the same protocol where the second

deletion ($\Delta 3850$) was constructed over the $\Delta 0242$ mutant.

Complementation of the mutant strains

The pWH1266-Km plasmid was constructed as previously described [68]. Then, in order to complement the $\Delta 0242$ strain, the A1S_0242 gene was amplified from the genome of the ATCC 17978 strain using primers listed in Table S2 and then cloned into the *EcoRV* and *BamHI* restriction sites of the pWH1266-Km plasmid under the control of the tetracycline resistance gene promoter using the primers listed in Table S2. The resulting construction was used to transform $\Delta 0242$ mutant cells by electroporation. Transformants were selected on kanamycin-containing plates and checked by PCR using primers listed in Table S2. Moreover, ATCC 17978 and $\Delta 0242$ strains harboring the empty pWH1266-Km vector were used as experimental controls. Finally, the $\Delta 3850$ derivative strain was also complemented following the same procedure described above.

Retrotranscription and real-time RT-PCR assays

Total RNA from ATCC 17978 strain and the isogenic mutants ($OD_{600} = 1.0$) was isolated using the High Pure RNA Isolation Kit (Roche, #11828665001). RNA samples were treated with DNase I (Invitrogen, #18068015) and purified with GeneJET RNA Cleanup and Concentration Micro Kit (Thermo Fisher Scientific, #K0841).

In order to analyze the polycistronic nature of the A1S_0242–0244 operon, the cDNA was obtained from RNA samples using the iScript cDNA Synthesis Kit (BioRad, #170–8890) following the manufacturer's recommendations. The cDNA from ATCC 17978 was amplified with the GoTaq G2 Flexi DNA Polymerase (Promega, #M7808) using pairs of primers designed to anneal to the 3'-end of every gene and the 5'-end of the next one (Table S2). Genomic DNA and total RNA without reverse transcription were used as templates for positive and negative controls, respectively, and the amplicons were detected by standard 1% agarose gel electrophoresis. The *gyrB* gene was used as a positive control. All the assays were performed in triplicate.

Real-time reverse transcription-PCR (qRT-PCR) was carried out to determine the expression level of the genes of interest using UPL (Roche) and TaqMan (Applied Biosystems) probes and primers listed in Table S2. The LightCycler 480 RNA Master hydrolysis probes kit (Roche, #04991885001) and the LightCycler 480 RNA instrument (Roche) were used together and the following protocol was used: initial incubation of 65 °C, 3 min, followed by a denaturation step at 95 °C for 30 s, 45 cycles

at 95 °C, 15 s and 60 °C, 45 s, and a final elongation step at 40 °C, 30 s. The expression level was standardized relative to the transcription level of the housekeeping gene *rpoB*. All the assays were performed in triplicate.

Growth curve analysis

Fitness was assessed by measuring the growth rates of the ATCC 17978 strain and the mutant derivatives strains. Briefly, 1.5 ml of LB medium were inoculated with approximately 5×10^7 CFU of each strain, previously grown until the stationary phase, and incubated at 37 °C with constant shaking at 180 rpm. Assays were performed in MH medium (*normal conditions*) and in MH supplemented with 200 μ M of 2,2'-bipyridyl (BIP, Sigma-Aldrich, #D216305) (*iron deficit conditions*). Growth was monitored using 24-well plates in an Epoch 2 Microplate Spectrophotometer (BioTek Instruments, Inc.) and OD_{600} values were recorded every 10 min. At least three independent experiments were performed for each strain. The growth rate constant (μ) was calculated on the basis of the exponential segment of the growth curve and defined as \ln_2/g , where g is the doubling time or mean generation time. The results were compared using Student's *t* test.

Quantitative biofilm assay

Biofilm formation was determined following the protocol previously described by Tomaras *et al.* [23] and modified by Alvarez-Fraga *et al.* [68]. Briefly, colonies of *A. baumannii* were grown on LB plates and used to inoculate LB broth. Overnight cultures were centrifuged and the pellet washed and resuspended in 5 mL of SB medium (0.5% NaCl and 1% tryptone). A 1:100 dilution of each sample was stagnant incubated at 37 °C for 48 h. In order to evaluate the total cell biomass the growth was measured at OD_{600} . Biofilm formation ability was analyzed by crystal violet staining followed by solubilisation with ethanol-acetone. In order to avoid variations due to differences in bacterial growth under different experimental conditions, the OD_{580}/OD_{600} ratio was used to normalize the amount of biofilm formed to the total cell content of each sample. Eight independent replicates were performed. Student's *t*-test was performed to evaluate the statistical significance of observed differences.

Adhesion to A549 human alveolar epithelial cells

The ability of the isogenic *A. baumannii* strains ($\Delta 0242$, $\Delta 3850$ and the double mutant $\Delta 0242/\Delta 3850$) to adhere to A549 human epithelial cells was evaluated and compared to the wild type strain. Invasion and adhesion

abilities were analyzed as previously described by Gaddy *et al.* [25] with some modifications [68]. Briefly, A549 human alveolar epithelial cells were grown at 37°C and 5% CO₂ in DMEM medium (Sigma-Aldrich, #D5671) containing 10% of fetal bovine serum (FBS) and 1% of penicillin-streptomycin (Gibco, #15070063). Monolayers were washed with saline solution and HBSS (Hank's balanced salt solution, Gibco, #11520476) without glucose (mHBSS). After that, A549 cells were infected with 10⁷ bacteria *per well* and incubated, 3 h for the adherence determination, in mHBSS at 37 °C. To analyze the attachment ability of bacteria, A549 cells were washed with saline solution and lysed in 500 μL of 0.5% sodium deoxycholate. Dilutions of the lysates were plated onto LB agar and incubated at 37 °C for 24 h. Colony forming units were counted to determine bacteria that had attached to or invaded A549 cells. Four independent replicates were done. Student's t-tests were performed to evaluate the statistical significance of the observed differences.

Determination of susceptibility to oxidative stress

The susceptibility to oxidative stress of the ATCC 17978 strain type and the isogenic mutant derivative strains was determined by microdilution using paraquat (Sigma-Aldrich, #856177) to achieve oxidative stress conditions in order to obtain the Minimal Inhibitory Concentration (MIC), following the CLSI criteria [70]. Briefly, strains were grown in MH plates for 24 h at 37°C. Then, 150 μL of serial dilutions of MH medium containing paraquat were performed in 96-well plates in the presence (100 μM) or absence of the metal chelator 2,2'-bipyridyl (BIP). Plates were then inoculated with 7.5 μL of a 0.5 McFarland cellular suspension containing approximately 1 × 10⁷ CFU/mL of bacteria. Bacterial growth on plates was studied after incubation at 37°C for 24 h.

***Galleria mellonella* virulence assay**

The virulence of the wild type strain and its derivative mutant strains was evaluated using a *G. mellonella* survival assay and a determination of the lethal doses (LD₅₀ and LD₁₀₀). Caterpillars were obtained from Bio Systems Technology (Exeter, UK) and stored at 15 °C prior to use. *A. baumannii* cells previously grown for 24 h in LB broth were collected by centrifugation and resuspended in sterile phosphate-buffered saline (PBS). Appropriate bacterial inocula were determined spectrophotometrically at OD₆₀₀ and confirmed by plate counting using LB agar plates. Thus, *G. mellonella* survival assays were performed by injecting 10 μL-suspension containing approximately 2 × 10⁴ CFU/larva in groups of 10 larvae

as previously described [71]. Two control groups were included; not injected larvae (intact) and larvae injected with an equivalent volume of sterile PBS. The tested groups included larvae infected with ATCC 17978, Δ0242, Δ3850 and Δ0242/Δ3850 strains. After injection, the larvae were incubated at 37°C in darkness, and death was assessed at 8 h intervals over 6 days. Caterpillars were considered dead and removed if they displayed no response to probing. The resulting survival curves were plotted using the Kaplan-Meier method [72] and analyzed using the log-rank (Mantel-Cox) test.

LD₅₀ and LD₁₀₀ were calculated using groups of 7 larvae of *G. mellonella* infected as described above. Larvae were infected with each strain with an inoculum of 10 μL starting at 8 × 10⁵ CFUs/larvae, and then the inocula serially diluted at 2 × 10⁵, 8 × 10⁴, 2.6 × 10⁴, 8 × 10³ and 2.6 × 10³ CFUs/larvae. Control groups were also included. Lethal doses were obtained for 24 and 144 h post-infection [73].

Murine pneumonia virulence assay

The pneumonia model was used to evaluate the virulence ability of the ATCC 17978 and the isogenic mutant Δ0242 strain using BALB/c male mice. The procedure followed was the above described for bacterial RNA extraction from the infection, with the exception of the euthanasia that occurred using an overdose of thiopental sodium 144 h after inoculation. Death was assessed at 8 h intervals. The survival curves were plotted using the Kaplan-Meier method [72] and analyzed using the log-rank (Mantel-Cox) test.

To ascertain the relevance of the *feoA* gene in virulence in mice pneumonia a second series of assays was performed to determine the effect of the inactivation of *feoA* on the bacterial load in lungs and presence of bacteria in blood. Groups of 12 mice were intratracheally inoculated as previously described with the ATCC 17978 and the mutant Δ0242 strains. Mice were inoculated with approximately 2 × LD₁₀₀ of the ATCC 17978 (12 × 10⁷ CFUs/mouse) and observed for mortality over 72 h. All the animals were analyzed immediately after death. Blood and lung samples were obtained and processed as previously described previously [74]. Student's t-test was performed to evaluate the statistical significance of differences.

Disclosure of potential conflicts of interest

No potential conflicts of interest were disclosed.

Acknowledgements

This work has been funded by Projects PI15/00860 to GB, CP13/00226 to AB, PI11/01034 to MP and P14/00059 and

PI17/01482 to MP and AB, all integrated in the National Plan for Scientific Research, Development and Technological Innovation 2013–2016 and funded by the ISCIII – General Subdirection of Assessment and Promotion of the Research-European Regional Development Fund (FEDER) “A way of making Europe”. The study was also funded by the project IN607A 2016/22 (Consellería de Cultura, Educación e Ordenación Universitaria) to G.B. Also supported by Planes Nacionales de I+D+i 2008–2011 / 2013–2016 and Instituto de Salud Carlos III, Subdirección General de Redes y Centros de Investigación Cooperativa, Ministerio de Economía y Competitividad, Spanish Network for Research in Infectious Diseases (REIPI RD12/0015/0014 and REIPI RD16/0016/006) cofinanced by European Development Regional Fund “A way to achieve Europe” and operative program Intelligent Growth 2014–2020. J. A. Vallejo was financially supported by the Sara Borrell Programme (ISCIII, Spain CD13/00373), J.C. Vázquez-Ucha was financially supported by the Miguel Servet Programme (ISCIII, Spain CP13/00226) and M. Martínez-Gutián was financially supported by the grant Clara Roy (Spanish Society of Clinical Microbiology and Infectious Diseases). We thank M. I. Voskuil (Dept. of Immunology and Microbiology, University of Colorado Medical School, CO, USA) for providing pMo130.

Funding

Consellería de Cultura, Educación y Ordenación Universitaria Xunta de Galicia-Spain, Miguel Servet program-ISCIII-Spain, Sara Borrell Program-ISCIII-Spain, REIPI-Spain, SEIMC-Spain, ISCIII-Spain.

References

- [1] Global priority list of antibiotic-resistant bacteria to guide research, discovery and development of new antibiotics. Geneva (Switzerland): World Health Organization. 2017.
- [2] Peleg AY, Seifert H, Paterson DL. *Acinetobacter baumannii*: emergence of a successful pathogen. *Clin Microbiol Rev.* 2008;21:538–82. doi:10.1128/CMR.00058-07.
- [3] Maragakis LL, Perl TM. *Acinetobacter baumannii*: epidemiology, antimicrobial resistance, and treatment options. *Clin Infect Dis.* 2008;46:1254–63. doi:10.1086/529198.
- [4] Gales AC, Jones RN, Sader HS. Contemporary activity of colistin and polymyxin B against a worldwide collection of Gram-negative pathogens: results from the SENTRY Antimicrobial Surveillance Program (2006–09). *J Antimicrob Chemother.* 2011;66:2070–4. doi:10.1093/jac/dkr239.
- [5] Karaiskos I, Souli M, Galani I, et al. Colistin: still a life-saver for the 21st century? *Expert Opin Drug Metab Toxicol.* 2017;13:59–71. doi:10.1080/17425255.2017.1230200.
- [6] Pournaras S, Koumaki V, Gennimata V, et al. In Vitro Activity of Tigecycline Against *Acinetobacter baumannii*: Global Epidemiology and Resistance Mechanisms. *Adv Exp Med Biol.* 2016;897:1–14.
- [7] Bou G, Cerveró G, Domínguez MA, et al. PCR-based DNA fingerprinting (REP-PCR, AP-PCR) and pulsed-field gel electrophoresis characterization of a nosocomial outbreak caused by imipenem- and meropenem-resistant *Acinetobacter baumannii*. *Clin Microbiol Infect.* 2000;6:635–43. doi:10.1046/j.1469-0691.2000.00181.x.
- [8] Higgins PG, Dammhayn C, Hackel M, et al. Global spread of carbapenem-resistant *Acinetobacter baumannii*. *J Antimicrob Chemother.* 2010;65:233–8. doi:10.1093/jac/dkp428.
- [9] Valencia R, Arroyo LA, Conde M, et al. Nosocomial outbreak of infection with pan-drug-resistant *Acinetobacter baumannii* in a tertiary care university hospital. *Infect Control Hosp Epidemiol.* 2009;30:257–63. doi:10.1086/595977.
- [10] Corbella X, Montero A, Pujol M, et al. Emergence and rapid spread of carbapenem resistance during a large and sustained hospital outbreak of multiresistant *Acinetobacter baumannii*. *J Clin Microbiol.* 2000;38:4086–95.
- [11] McConnell MJ, Actis L, Pachón J. *Acinetobacter baumannii*: human infections, factors contributing to pathogenesis and animal models. *FEMS Microbiol Rev.* 2013;37:130–55. doi:10.1111/j.1574-6976.2012.00344.x.
- [12] Smani Y, Dominguez-Herrera J, Pachón J. Association of the outer membrane protein Omp33 with fitness and virulence of *Acinetobacter baumannii*. *J Infect Dis.* 2013;208:1561–70. doi:10.1093/infdis/jit386.
- [13] Lee JC, Koerten H, van den Broek P, et al. Adherence of *Acinetobacter baumannii* strains to human bronchial epithelial cells. *Res Microbiol.* 2006;157:360–6. doi:10.1016/j.resmic.2005.09.011.
- [14] Pérez A, Merino M, Rumbo-Feal S, et al. The FhaB/FhaC two-partner secretion system is involved in adhesion of *Acinetobacter baumannii* AbH12O-A2 strain. *Virulence.* 2017;8(6):959–974. doi:10.1080/21505594.
- [15] Méndez JA, Mateos J, Beceiro A, et al. Quantitative proteomic analysis of host–pathogen interactions: a study of *Acinetobacter baumannii* responses to host airways. *BMC Genomics.* 2015;16:422. doi:10.1186/s12864-015-1608-z.
- [16] Merino M, Alvarez-Fraga L, Gomez MJ, et al. Complete Genome Sequence of the Multiresistant *Acinetobacter baumannii* Strain AbH12O-A2, Isolated during a Large Outbreak in Spain. *Genome Announc.* 2014;2: doi:10.1128/genomeA.01182-14.
- [17] Acosta J, Merino M, Viedma E, et al. Multidrug-resistant *Acinetobacter baumannii* Harboring OXA-24 carbapenemase, Spain. *Emerg Infect Dis.* 2011;17:1064–7. doi:10.3201/eid1706.091866.
- [18] Gaddy JA, Arivett BA, McConnell MJ, et al. Role of acinetobactin-mediated iron acquisition functions in the interaction of *Acinetobacter baumannii* strain ATCC 19606T with human lung epithelial cells, *Galleria mellonella* caterpillars, and mice. *Infect Immun.* 2012;80:1015–24. doi:10.1128/IAI.06279-11.
- [19] Mendez JA, Soares NC, Mateos J, et al. Extracellular proteome of a highly invasive multidrug-resistant clinical strain of *Acinetobacter baumannii*. *J Proteome Res.* 2012;11:5678–94. doi:10.1021/pr300496c.
- [20] Loehfelm TW, Luke NR, Campagnari AA. Identification and characterization of an *Acinetobacter baumannii* biofilm-associated protein. *J Bacteriol.* 2008;190:1036–44. doi:10.1128/JB.01416-07.
- [21] Choi AH, Slamti L, Avci FY, et al. The pgaABCD locus of *Acinetobacter baumannii* encodes the production of poly-beta-1–6-N-acetylglucosamine, which is critical for

- biofilm formation. *J Bacteriol.* **2009**;191:5953–63. doi:10.1128/JB.00647-09.
- [22] Tomaras AP, Flagler MJ, Dorsey CW, et al. Characterization of a two-component regulatory system from *Acinetobacter baumannii* that controls biofilm formation and cellular morphology. *Microbiology.* **2008**;154:3398–409. doi:10.1099/mic.0.2008/019471-0.
- [23] Tomaras AP, Dorsey CW, Edelmann RE, et al. Attachment to and biofilm formation on abiotic surfaces by *Acinetobacter baumannii*: involvement of a novel chaperone-usher pili assembly system. *Microbiology.* **2003**;149:3473–84. doi:10.1099/mic.0.26541-0.
- [24] de Brij A, Gaddy J, van der Meer J, et al. CsuA/BABCDE-dependent pili are not involved in the adherence of *Acinetobacter baumannii* ATCC19606(T) to human airway epithelial cells and their inflammatory response. *Res Microbiol.* **2009**;160:213–8. doi:10.1016/j.resmic.2009.01.002.
- [25] Gaddy JA, Tomaras AP, Actis LA. The *Acinetobacter baumannii* 19606 OmpA protein plays a role in biofilm formation on abiotic surfaces and in the interaction of this pathogen with eukaryotic cells. *Infect Immun.* **2009**;77:3150–60. doi:10.1128/IAI.00096-09.
- [26] Dashner SG, Butler CA, Lissel JP, et al. A novel *Porphyromonas gingivalis* FeoB plays a role in manganese accumulation. *J Biol Chem.* **2005**;280:28095–102. doi:10.1074/jbc.M503896200.
- [27] Nairz M, Schroll A, Sonnweber T, et al. The struggle for iron – a metal at the host-pathogen interface. *Cell Microbiol.* **2010**;12:1691–702. doi:10.1111/j.1462-5822.2010.01529.x.
- [28] Chu BC, Garcia-Herrero A, Johanson TH, et al. Siderophore uptake in bacteria and the battle for iron with the host; a bird's eye view. *Biometals.* **2010**;23:601–11. doi:10.1007/s10534-010-9361-x.
- [29] Proschak A, Lubuta P, Grun P, et al. Structure and biosynthesis of fimsbactins A-F, siderophores from *Acinetobacter baumannii* and *Acinetobacter baylyi*. *Chembiochem.* **2013**;14:633–8. doi:10.1002/cbic.201200764.
- [30] Penwell WF, DeGrace N, Tentarelli S, et al. Discovery and Characterization of New Hydroxamate Siderophores, Baumannoferrin A and B, produced by *Acinetobacter baumannii*. *Chembiochem.* **2015**;16:1896–1904. doi:10.1002/cbic.201500147.
- [31] Shapiro JA, Wenciewicz TA. Acinetobactin Isomerization Enables Adaptive Iron Acquisition in *Acinetobacter baumannii* through pH-Triggered Siderophore Swapping. *ACS Infect Dis.* **2016**;2:157–68. doi:10.1021/acinfecdis.5b00145.
- [32] Weaver EA, Wyckoff EE, Mey AR, et al. FeoA and FeoC are essential components of the *Vibrio cholerae* ferrous iron uptake system, and FeoC interacts with FeoB. *J Bacteriol.* **2013**;195:4826–35. doi:10.1128/JB.00738-13.
- [33] Naikare H, Palyada K, Panciera R, et al. Major role for FeoB in *Campylobacter jejuni* ferrous iron acquisition, gut colonization, and intracellular survival. *Infect Immun.* **2006**;74:5433–44. doi:10.1128/IAI.00052-06.
- [34] Mortensen BL, Skaar EP. The contribution of nutrient metal acquisition and metabolism to *Acinetobacter baumannii* survival within the host. *Front Cell Infect Microbiol.* **2013**;3:95. doi:10.3389/fcimb.2013.00095.
- [35] Runyen-Janecky LJ, Reeves SA, Gonzales EG, et al. Contribution of the Shigella flexneri Sit, Iuc, and Feo iron acquisition systems to iron acquisition *in vitro* and in cultured cells. *Infect Immun.* **2003**;71:1919–28. doi:10.1128/IAI.71.4.1919-1928.2003.
- [36] Robey M, Cianciotto NP. Legionella pneumophila feoAB promotes ferrous iron uptake and intracellular infection. *Infect Immun.* **2002**;70:5659–69. doi:10.1128/IAI.70.10.5659-5669.2002.
- [37] Velayudhan J, Hughes NJ, McColm AA, et al. Iron acquisition and virulence in *Helicobacter pylori*: a major role for FeoB, a high-affinity ferrous iron transporter. *Mol Microbiol.* **2000**;37:274–86. doi:10.1046/j.1365-2958.2000.01987.x.
- [38] Stojiljkovic I, Cobeljic M, Hantke K. Escherichia coli K-12 ferrous iron uptake mutants are impaired in their ability to colonize the mouse intestine. *FEMS Microbiol Lett.* **1993**;108:111–5. doi:10.1111/j.1574-6968.1993.tb06082.x.
- [39] Boyer E, Bergevin I, Malo D, et al. Acquisition of Mn(II) in addition to Fe(II) is required for full virulence of *Salmonella enterica* serovar Typhimurium. *Infect Immun.* **2002**;70:6032–42. doi:10.1128/IAI.70.11.6032-6042.2002.
- [40] Kammler M, Schön C, Hantke K. Characterization of the ferrous iron uptake system of *Escherichia coli*. *J Bacteriol.* **1993**;175:6212–9. doi:10.1128/jb.175.19.6212-6219.1993.
- [41] Stevenson B, Wyckoff EE, Payne SM. *Vibrio cholerae* FeoA, FeoB, and FeoC Interact To Form a Complex. *J Bacteriol.* **2016**;198:1160–70. doi:10.1128/JB.00930-15.
- [42] Hantke K. Regulation of ferric iron transport in *Escherichia coli* K12: isolation of a constitutive mutant. *Mol Gen Genet.* **1981**;182:288–92. doi:10.1007/BF00269672.
- [43] Hantke K. Ferrous Iron Transport, p 178–184. In: Crosa J, Mey A, Payne S, editors. *Iron Transport in Bacteria*. Washington, DC: ASM Press; **2004**. doi:10.1128/9781555816544.ch12.
- [44] Hantke K. Selection procedure for deregulated iron transport mutants (fur) in *Escherichia coli* K 12: fur not only affects iron metabolism. *Mol Gen Genet.* **1987**;210:135–9. doi:10.1007/BF00337769.
- [45] Cartron ML, Maddocks S, Gillingham P, et al. Feo-transport of ferrous iron into bacteria. *Biometals.* **2006**;19:143–57. doi:10.1007/s10534-006-0003-2.
- [46] Subashchandrabose S, Smith S, DeOrnellas V, et al. *Acinetobacter baumannii* Genes Required for Bacterial Survival during Bloodstream Infection. *mSphere.* **2015**;1: doi:10.1128/mSphere.00013-15.
- [47] Antunes LC, Imperi F, Towner KJ, et al. Genome-assisted identification of putative iron-utilization genes in *Acinetobacter baumannii* and their distribution among a genotypically diverse collection of clinical isolates. *Res Microbiol.* **2011**;162:279–84. doi:10.1016/j.resmic.2010.10.010.
- [48] Beceiro A, Tomas M, Bou G. Antimicrobial resistance and virulence: a successful or deleterious association in the bacterial world? *Clin Microbiol Rev.* **2013**;26:185–230. doi:10.1128/CMR.00059-12.
- [49] Dorsey CW, Beglin MS, Actis LA. Detection and analysis of iron uptake components expressed by *Acinetobacter baumannii* clinical isolates. *J Clin Microbiol.* **2003**;41:4188–93. doi:10.1128/JCM.41.9.4188-4193.2003.
- [50] Catel-Ferreira M, Marti S, Guillon L, et al. The outer membrane porin OmpW of *Acinetobacter baumannii* is

- involved in iron uptake and colistin binding. *FEBS Lett.* **2016**;590:224–31. doi:10.1002/1873-3468.12050.
- [51] Catel-Ferreira M, Nehme R, Molle V, et al. Deciphering the function of the outer membrane protein OprD homologue of *Acinetobacter baumannii*. *Antimicrob Agents Chemother.* **2012**;56:3826–32. doi:10.1128/AAC.06022-11.
- [52] Murray GL, Tsyganov K, Kostoulias XP, et al. Global gene expression profile of *Acinetobacter baumannii* during bacteremia. *J Infect Dis.* **2017**;215:S52–7. doi:10.1093/infdis/jiw529.
- [53] Miethke M, Marahiel MA. Siderophore-based iron acquisition and pathogen control. *Microbiol Mol Biol Rev.* **2007**;71:413–51. doi:10.1128/MMBR.00012-07.
- [54] Zimblar DL, Penwell WF, Gaddy JA, et al. Iron acquisition functions expressed by the human pathogen *Acinetobacter baumannii*. *Biometals.* **2009**;22:23–32. doi:10.1007/s10534-008-9202-3.
- [55] Harding RA, Royt PW. Acquisition of iron from citrate by *Pseudomonas aeruginosa*. *J Gen Microbiol.* **1990**;136:1859–67. doi:10.1099/00221287-136-9-1859.
- [56] Ratledge C, Dover LG. Iron metabolism in pathogenic bacteria. *Annu Rev Microbiol.* **2000**;54:881–941. doi:10.1146/annurev.micro.54.1.881.
- [57] Marshall B, Stintzi A, Gilmour C, et al. Citrate-mediated iron uptake in *Pseudomonas aeruginosa*: involvement of the citrate-inducible FecA receptor and the FeoB ferrous iron transporter. *Microbiology.* **2009**;155:305–15. doi:10.1099/mic.0.023531-0.
- [58] Ganne G, Brillet K, Basta B, et al. Iron Release from the Siderophore Pyoverdine in *Pseudomonas aeruginosa* Involves Three New Actors: FpvC, FpvG, and FpvH. *ACS Chem Biol.* **2017**;12:1056–65. doi:10.1021/acscchembio.6b01077.
- [59] Louvel H, Saint Girons I, Picardeau M. Isolation and characterization of FecA- and FeoB-mediated iron acquisition systems of the spirochete *Leptospira biflexa* by random insertional mutagenesis. *J Bacteriol.* **2005**;187:3249–54. doi:10.1128/JB.187.9.3249-3254.2005.
- [60] Sahl JW, Gillece JD, Schupp JM, et al. Evolution of a pathogen: a comparative genomics analysis identifies a genetic pathway to pathogenesis in *Acinetobacter*. *PLoS One.* **2013**;8:e54287. doi:10.1371/journal.pone.0054287.
- [61] Rumbo-Feal S, Gomez MJ, Gayoso C, et al. Whole transcriptome analysis of *Acinetobacter baumannii* assessed by RNA-sequencing reveals different mRNA expression profiles in biofilm compared to planktonic cells. *PLoS One.* **2013**;8:e72968. doi:10.1371/journal.pone.0072968.
- [62] Eijkelkamp BA, Hassan KA, Paulsen IT, et al. Investigation of the human pathogen *Acinetobacter baumannii* under iron limiting conditions. *BMC genomics.* **2011**;12:126. doi:10.1186/1471-2164-12-126.
- [63] Miller AF. Superoxide dismutases: ancient enzymes and new insights. *FEBS Lett.* **2012**;586:585–95. doi:10.1016/j.febslet.2011.10.048.
- [64] Lenski RE. Quantifying fitness and gene stability in microorganisms. *Biotechnology.* **1991**;15:173–92.
- [65] Madigan MT MJ, Dunlap PV, Clark DP. *Brock biology of microorganisms*. 12th ed. Texas, USA: Pearson Education Inc. **2009**.
- [66] Hassett DJ, Cohen MS. Bacterial adaptation to oxidative stress: implications for pathogenesis and interaction with phagocytic cells. *FASEB J.* **1989**;3:2574–82.
- [67] Rumbo-Feal S, Perez A, Ramelot TA, et al. Contribution of the *A. baumannii* AIS_0114 Gene to the Interaction with Eukaryotic Cells and Virulence. *Front Cell Infect Microbiol.* **2017**;7:108. doi:10.3389/fcimb.2017.00108.
- [68] Álvarez-Fraga L, Pérez A, Rumbo-Feal S, et al. Analysis of the role of the LH92_11085 gene of a biofilm hyper-producing *Acinetobacter baumannii* strain on biofilm formation and attachment to eukaryotic cells. *Virulence.* **2016**;7:443–55. doi:10.1080/21505594.2016.1145335.
- [69] Hamad MA, Zajdowicz SL, Holmes RK, et al. An allelic exchange system for compliant genetic manipulation of the select agents *Burkholderia pseudomallei* and *Burkholderia mallei*. *Gene.* **2009**;430:123–31. doi:10.1016/j.gene.2008.10.011.
- [70] CLSI W, PA, USA. *Methods for Dilution Antimicrobial Susceptibility Tests for Bacteria that Grow Aerobically—Tenth Edition: Approved Standard M07-A10, 2015*.
- [71] Hornsey M, Longshaw C, Phee L, et al. *In vitro* activity of telavancin in combination with colistin versus Gram-negative bacterial pathogens. *Antimicrob Agents Chemother.* **2012**;56:3080–5. doi:10.1128/AAC.05870-11.
- [72] Kaplan EL, Meier P. Nonparametric Estimation from Incomplete Observations. *J Am Statist Assoc.* **1958**;53:457–81. doi:10.1080/01621459.1958.10501452.
- [73] Lopez-Rojas R, Dominguez-Herrera J, McConnell MJ, et al. Impaired virulence and *in vivo* fitness of colistin-resistant *Acinetobacter baumannii*. *J Infect Dis.* **2011**;203:545–8. doi:10.1093/infdis/jiq086.
- [74] Rodriguez-Hernandez MJ, Pachon J, Pichardo C, et al. Imipenem, doxycycline and amikacin in monotherapy and in combination in *Acinetobacter baumannii* experimental pneumonia. *J Antimicrob Chemother.* **2000**;45:493–501. doi:10.1093/jac/45.4.493.